Journal of Molecular Histology (2021) 52:1189–1204
https://doi.org/10.1007/s10735-021-10032-y

ORIGINAL PAPER

The vascularization, innervation and myogenesis of early regenerated tail in *Gekko japonicus*

Zhuang Liu[1] · Shuai Huang[1] · Man Xu[1] · Wenxue Zhang[1] · Tuchen Guan[1] · Qinghua Wang[1] · Mei Liu[1] · Jian Yao[2] · Yan Liu[1]

Received: 23 February 2021 / Accepted: 16 October 2021 / Published online: 21 October 2021
© The Author(s), under exclusive licence to Springer Nature B.V. 2021

Abstract

Many species of lizards are capable of tail regeneration. There has been increased interest in the study of lizard tail regeneration in recent years as it is an amenable regeneration model for amniotes. In this study, *Gekko japonicus* was used as a model to investigate the initiation of vascularization, innervation and myogenesis during tail regeneration. We found that angiogenesis and axon regeneration occurred almost simultaneously within 4 days post amputation. The results showed that the endothelial cells of the original vasculature proliferated and extended into the blastema as capillary vessels, which inter-connected to form a capillary network. The nerve fibers innervated the regenerated tissue from the original spinal cord and dorsal root ganglia, and the fiber bundles increased during 14 days. Regenerating muscle tissues emerged 2 weeks after amputation. PAX3 and PAX7 expression were detected during myogenesis, with PAX7 showing a continuous increase in expression from day 3 until the day 14, whereas PAX3 reached a peak level on day 10 day post amputation, and then declined quickly to level as normal control on day 14. PCNA and PAX3 double-positive satellite cells were observed in the original rostral tissues, indicating the involvement of satellite cell proliferation during tail regeneration. Taken together, these data suggest that tail regeneration in *Gekko japonicus* involved rapid angiogenesis from the beginning to the day 10 and followed by capillary remodeling. The innervation of regenerated tail was significant on day 4 and increased gradually during regeneration, while the regenerated muscle tissues was obvious on day 14 after amputation.

Keywords Tail regeneration · *Gekko japonicus* · Angiogenesis · Innervation · Myogenesis · PAX3

Introduction

Many amphibians and reptiles have the capacity for appendage regeneration. For example, salamanders regenerate limbs (Haas and Whited 2017; Nowoshilow et al. 2018) and lizards regenerate their tails (Alibardi 2014; McLean and Vickaryous 2011). The initiation and progression of regeneration have been investigated extensively in axolotl and zebrafish (Haas and Whited 2017; Pfefferli and Jaźwińska 2015), whereas it is less well studied in lizards. However, the study of lizard tail regeneration has attracted increasing interest as an amenable model for regeneration amniotes, and various studies on tail regeneration have been reported in different species, including *Anolis carolinensis* (Zika 1969; Fisher et al. 2012; Lozito and Tuan 2015; Hutchins et al. 2014), *Eublepharis macularius* (McLean and Vickaryous 2011; Delorme et al. 2012), *Podarcis muralis* (Alibardi 2014), and *Gekko japonicus* (Zhou et al. 2013).

The original reptile tail is a complex appendage composed of vasculature, nervous tissue, muscle, skeletal and adipose tissues. The process of regeneration comprises sequential events, including an early wound-healing response involving re-epithelialization of the transection site by the adjacent wounded epithelium and blastema formation (Gilbert et al. 2013; Xu et al. 2019). The differentiated tissues of the regenerated tail are derived from heterogeneous blastemal

✉ Jian Yao
yjshz@ntu.edu.cn

✉ Yan Liu
liuyan@ntu.edu.cn

[1] Key Laboratory of Neuroregeneration of Jiangsu Province and Ministry of Education, Co-Innovation Center of Neuroregeneration, Nantong University, Nantong 226001, Jiangsu Province, China

[2] Department of Histology and Embryology, Medical School of Nantong University, Nantong 226001, Jiangsu Province, China

cells, which have been proposed to originate from either dedifferentiated tissues or tissue-specific adult progenitor cells (Stocum and Cameron 2011; Nacu and Tanaka 2011). The regenerated appendage of axolotl or lizard is capable of generating de novo muscle tissues, which is the largest volume tissue in both original and regenerated tails. While the source of muscle cells remains elusive (Sandoval-Guzmán et al. 2014; Morrison et al. 2006; Kahn and Simpson 1974; Londono et al. 2017) the resident myogenic satellite cells have been proposed to be the main contributor to regenerated muscles (Kahn and Simpson 1974; Hutchins et al. 2014).

Various studies, describing the gross morphological view of regenerated tail at different stages, have provided valuable information about the innervation and vascularization of the regenerated tail. The critical role of innervation in appendage regeneration has been demonstrated in many species (Haas and Whited 2017; Pfefferli and Jaźwińska 2015; Yokoyama 2008). Consistent with this, axons innervating the tail blastema in lizards are derived from the proximal portion of the original spinal cord and dorsal root ganglia (Simpson 1970). Similarly, vascularization of regenerated tissue is essential for successful regeneration. Vascularization usually includes angiogenesis and vasculogenesis (Semenza 2007), where angiogenesis refers to the growth of endothelial sprouts from pre-existing vessels, and vasculogenesis refers to de novo blood vessel formation. While blood vessel formation has been described in the regenerating tail of leopard gecko (Payne et al. 2017), previous studies have predominantly focused on comparing the state of innervation and vascularization in the fully regenerated tail with the original tail and there is a lack detailed information about the progress of the innervation and vascularization during the initial 2 weeks post amputation. Moreover, the relationship between regenerating nerves and vessels has not been extensively addressed in lizards.

In this study, we investigated in detail the temporal and spatial relationship of renascent nerves and vessels within the first 2 weeks after amputation. We have also described the process of muscle regeneration and maturation, and determined whether muscle satellite cells were activated to proliferate during tail regeneration in *Gekko japonicus*. These results provide a detailed description of the relationships between innervation, vascularization and myogenesis during tail regeneration and provide a basis for further studies of molecular mechanisms that underlie these processes.

Materials and methods

Animals

Adult *Gekko japonicus* were collected from the Laboratory Animal Center of Nantong University. *Gekko japonicus* were freely fed with mealworms, aerated water and housed in an air-conditioned room with controlled temperature (26–28 °C). The experimental protocols were approved by the Laboratory Animal Care and Use Committee of the Nantong University (S20190405-402). A total of 42 geckos (50% male: female) with a mean body length (including tail) of 11.25 ± 0.6455 cm (mean ± SD) were used in this study. To mimic autotomy in the natural environment, caudotomy was performed at the sixth tail segment by inserting a nylon slipknot and pulling gently to remove the tail (Jiang et al. 2009).

Immunofluorescence

For immunofluorescence analyses, regenerate tail samples (n = 25) were collected from 5 geckos at each time point (4, 7, 10, 12, 14 days) after amputation. Geckos were anesthetized by freezing on ice for two minutes before the blastema was collected by making an incision 5 mm rostral to the amputation plane. Tissues were fixed in 4% PFA with 0.1 M phosphate buffered saline (PBS) for 4 h before being washed with 0.01 M PBS for three times with 10 min each washing. The samples were then cryo-protected in increasing concentrations of sucrose (5%, 10%, 20%, and 30%) before being frozen in Tissue-Tek OCT compound (Sakura Finetek USA) and cryosectioned (12 μm). Frozen sections were stored at − 80 °C. Thawed sections of blastema were permeabilized with 0.5% Triton X-100, blocked with 10% bovine serum albumin in 0.01 M PBS for 1 h at 37 °C and subsequently incubated overnight at 4 °C with primary antibodies: anti-CD34 for endothelial cell, anti-Tuj1 for neuron, anti-MHC for muscular cell, anti-PCNA and anti-BrdU for proliferating cell, anti-PAX3 for satellite cell. In some immunofluorescence experiments, the mouse anti-Tuj1 antibody was replaced by a rabbit anti-GAP43 antibody to permit double-labelling with the mouse anti-MHC antibody. The detailed information was listed in Table 1. After washing in 0.01 M PBS, the sections were further incubated with secondary antibodies for 2 h at RT and counterstained with Hoechst 33342 (1 μg/ml) (C1022, Beyotime Biotechnology, Shanghai, China) in 0.01 M PBS for 10 min. Fluorescence images

Table 1 Antibodies used in immunofluorescence (IF) and Western blot (WB). -P means primary antibody, and—S means secondary antibody

Application	Name	Host	Dilution	Vendor	RRID	Cat Num
IF-P	CD34	Rabbit	1:200	Abcam	AB_1640331	ab81289
IF-P	Tuj1	Mouse	1:200	Biolegend	AB_10063408	801202
IF-P	MHC	Mouse	1:200	R and D systems	AB_1293549	MAB4470
IF-P	PCNA	Rabbit	1:200	Cell Signaling Technology	AB_2636979	13110
IF-P	Gap43	Rabbit	1:200	Proteintech	AB_2278881	16971-1-AP
IF-P	PAX3	Mouse	1:200	R and D systems	AB_2159398	MAB2457
IF-P	BrdU	Mouse	1:200	Cell Signaling Technology	AB_10548898	5292
WB-P	PAX3	Rabbit	1:1000	Signalway	AB_2891226	32380
WB-P and IF-P	PAX7	Rabbit	1:1000	Aviva Systems Biology	AB_387565	ARP32742_P050
WB-P	β-actin	Mouse	1:1000	Abclonal	AB_2737399	AC004
IF-S	Alexa Flour 488-conjugated AffiniPure Goat Anti-Rabbit IgG (H+L)	Goat	1:1000	Jackson ImmunoResearch Labs	AB_2338046	111-545-003
IF-S	Alexa Flour Cy3-conjugated AffiniPure Goat Anti-mouse IgG (H+L)	Goat	1:1000	Jackson ImmunoResearch Labs	AB_2338680	115-165-003
WB-S	HRP conjugated Goat Anti-Rabbit IgG (H+L)	Goat	1:1000	Beyotime	AB_2892644	A0208
WB-S	HRP conjugated Goat Anti-mouse IgG (H + L)	Goat	1:1000	Beyotime	AB_2860575	A0216

were captured using a Zeiss Axio Imager M2 microscope, and analyzed using Image Pro Plus (Media Cybernetics, Rockville, MD) to quantify the relative levels of immunofluorescence signals.

Hematoxylin–eosin (HE) staining

Frozen sections of the regenerate tail samples (see above) were stained with hematoxylin and eosin (H&E) using a commercial kit (Beijing Solarbio Science, G1120). Briefly, frozen sections were thawed at 37 °C for 30 min, rinsed with deionized water (ddH2O, 5 min) and stained with Mayer's hematoxylin for 2.5 min at room temperature. Following rinses in running water (5 min) sections were treated with 10% HCl in 90% ethanol for 10 s, washed in water for 30 min and then stained in eosin for 1 min. Sections were subsequently dehydrated in increasing ethanol solutions (50%, 75%, 95% and 2 × 100% ethanol) and 3 changes in xylene (1.5 min each), before being cover-slipped and imaged.

BrdU incorporation assay

To label proliferating cells in S phase, 15 geckos (5 animals each collected at 10, 12 and 14 days after tail amputation) were injected intraperitoneally with 20 µl of 20 mM BrdU (5-bromo-2′-deoxyuridine, B5002, Sigma) diluted in phosphate-buffered saline (PBS) daily for two days before harvesting the regenerating tails. BrdU will be incorporated into all mitotically active cells within the time window of treatment, and will also be maintained in their progeny that don't divide. The samples were fixed and frozen as described above in the immunofluorescence assay. To detect incorporated BrdU, frozen sections were warmed for 30 min at 37 °C and rinsed with 0.01 M PBS before being treated with 1.5 M HCl for 30 min at 37 °C. After PBS washes and neutralization in 0.02 mM sodium tetraborate solution for 10 min at room temperature (25 °C), sections were blocked with 10% normal goat serum in 0.01 M PBS for 2 h at 37 °C

and incubated with anti-BrdU primary antibody overnight at 4 °C. Following PBS rinses, sections were incubated with the appropriate secondary fluorescently labelled antibody (Table 1) for 2 h at RT, counter-stained with 1ug/ml Hoechst 33342 (C1022, Beyotime Biotechnology, Shanghai, China) in 0.01 M PBS for 15 min at RT before being cover-slipped, imaged and analyzed as described above.

Western blot analysis

To investigate the levels of PAX3 and PAX7 proteins in regenerated tails at days 0, 3, 7 and 14 after amputation, tail samples, comprising 2 mm tail tissue rostral to the plane of autotomy together with the regenerated tissue, were collected from 3 geckos at each time point for western blotting. Total proteins were isolated from each sample by homogenizing in RIPA Lysis buffer (P0013B, Beyotime) containing 1 mM PMSF (ST506, Beyotime). After centrifugation at 12,000/min for 5 min, proteins were quantified with BCA reagents (P0011, Beyotime) and separated using sodium dodecyl sulfate–polyacrylamide gel electrophoresis (SDS-PAGE). The proteins were then transferred onto polyvinylidene fluoride (PVDF) membranes and incubated separately with PAX3 or PAX7 antibodies (detailed information showed in Table 1. The mouse anti-β-actin antibody was used as an internal control. Then, the membranes were incubated with horseradish peroxidase-conjugated secondary antibody at 25 °C for 2 h. The bands were visualized using chemiluminescence and quantified using Image Pro Plus (Media Cybernetics).

Statistics

All data are presented as mean ± SD values. The data were analyzed by One-way ANOVA followed by Bonferroni post-hoc test using SPSS Statistics 22.0 (SPSS Inc., Chicago, IL, USA). $p < 0.05$ was considered statistically significant.

Results

Rapid angiogenesis occurs in early regenerating tails

Tail regeneration begins with wound healing by the skin epithelium to re-cover the amputation site. Firstly, we documented the morphology of the regenerated tail on 4th, 7th, 10th and 14th day post amputation by HE staining (Supplementary Fig. S1) and found that the sequential events, including wound-healing and thickening by the epithelial covering, blastema formation and growth were similar to those in the leopard gecko, *Eublepharis macularius* (McLean and Vickaryous 2011). As the newly formed cell mass grows, neovascularization becomes necessary for further tissue formation and growth. To investigate the process of vascularization from 4th day to 14th day post amputation, we used CD34, which is a pan-endothelial marker expressed on early and mature vascular endothelial cells (Rakocevic et al. 2017), and showed that the endothelium of both rostral and caudal blood vessels were labelled with the CD34 antibody (Fig. 1). We observed that the vessels initially retracted from the amputation plane on day 4 (Fig. 1A), but by day 7 had grown towards the amputation plane (Fig. 1B). The vessels crossed the amputation plane into the newly formed blastema between days 7 and 12 (Fig. 1C) and from days 12 to 14 started to form a capillary network (Fig. 1C, D).

To identify proliferating endothelial cells, we co-labelled sections for incorporated BrdU, CD34 and with nuclear Hoechst dye (Fig. 2A–G). The BrdU and CD34 double-positive cells on 12th day are clearly evident at higher magnification in triple labelled images (Fig. 2H, inset), indicating that endothelial cells in the blastema of the tail proliferated during regeneration. Similar proliferating endothelial cells were also detected in proximal and distal regions of regenerate tail on the 10th and 14th days (Supplementary Fig. S2). We further found evidence for endothelial cells budding and migrating from existing blood vessels in cross sections of the blastema (Fig. 3). From days 10 to 14 post amputation, it can be clearly seen that the regular rounded capillary vessels gradually transform into an anastomosing reticular network of capillaries.

Rapid innervation of the early blastema

The innervation of the regenerating lizard tail was previously studied in *Podarcis muralis* (Alibardi and Miolo 1990) and, consistent with an earlier study (Simpson 1970), demonstrated that axons in the regenerate tail were derived from the original spinal cord and dorsal root ganglia rostral to amputation plane. In our study, we examined the time-course of blastema re-innervation using a Tuj1 antibody to detect the nerve fibers in double-labeling immunofluorescence experiments with CD34 antibody to

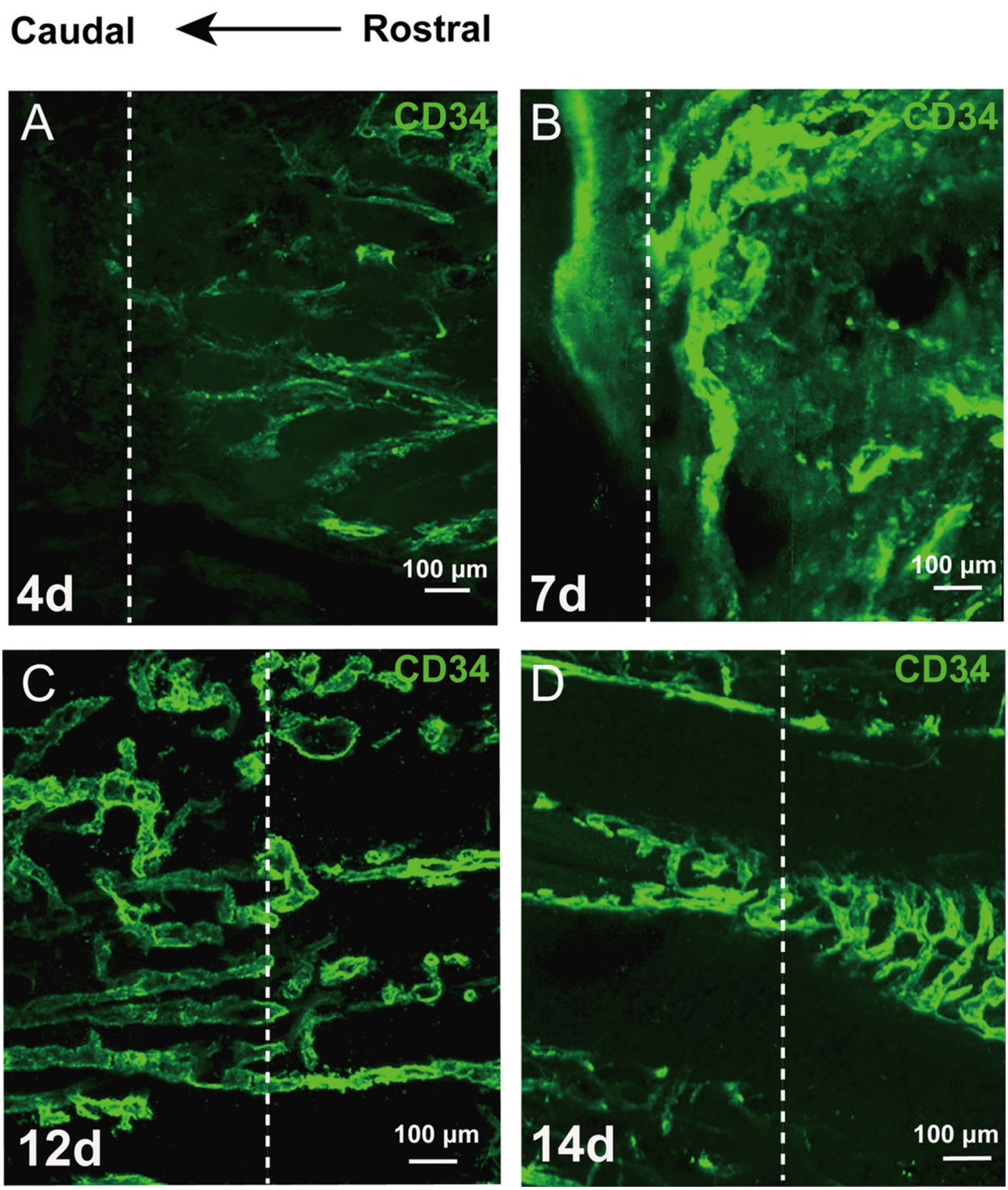

Fig. 1 Progression of angiogenesis in the regenerating blastema. Sections of the regenerate blastema at 4 days (**A**), 7 days (**B**), 12 days (**C**) and 14 days (**D**) post amputation, showing endothelial cells labelled with CD34 antibody. **A** At 4 days, the original vessels appeared to withdraw within the rostral stump. **B** By 7 days after amputation, regenerating vessels had reached the plane of truncation where the blastema started to form. **C** At 12 days, numerous regenerating vessels had traversed the amputation plane and by 14 days developed into an anastomosing capillary network. Dashed lines indicate amputation plane. Scale bar represents 100 µm

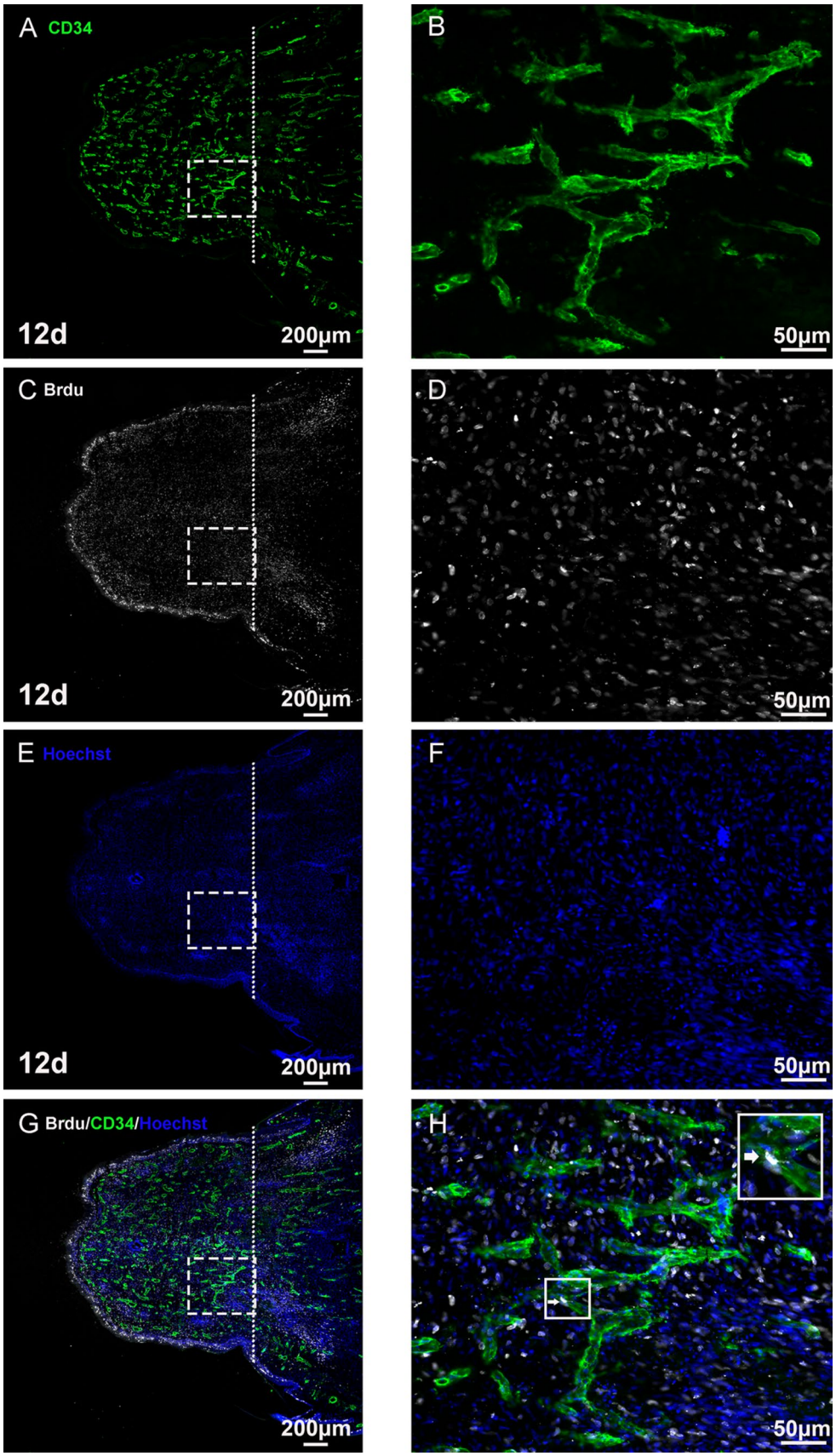

Fig. 2 Endothelial cell proliferation on 12th day post amputation. Co-labelling of sections with antibodies against CD34 (**A**, **B**, **G**, **H**), BrdU (**C**, **D**, **G**, **H**) and staining of nuclei with Hoechst dye (**E**, **F**) revealed proliferating endothelial cells (arrows in **H** and inset) in the abundant vessels present in blastema of the regenerating tail. **A**, **C**, **E** show single channels of CD34, BrdU and Hoechst staining at low power respectively, and G shows the merged view. Enlarged views of boxed areas in **A**, **C**, **E**, **G** are shown in **B**, **D**, **F** and **H** and further enlarged view of proliferating cells (arrows, $BrdU^{+}$/$CD34^{+}$) in boxed area of **G** are shown in the inset. Dashed lines indicate amputation plane. Scale bar represents 200 μm in **A**, **C**, **E** and **G**, 50 μm in **B**, **D**, **F** and **H**

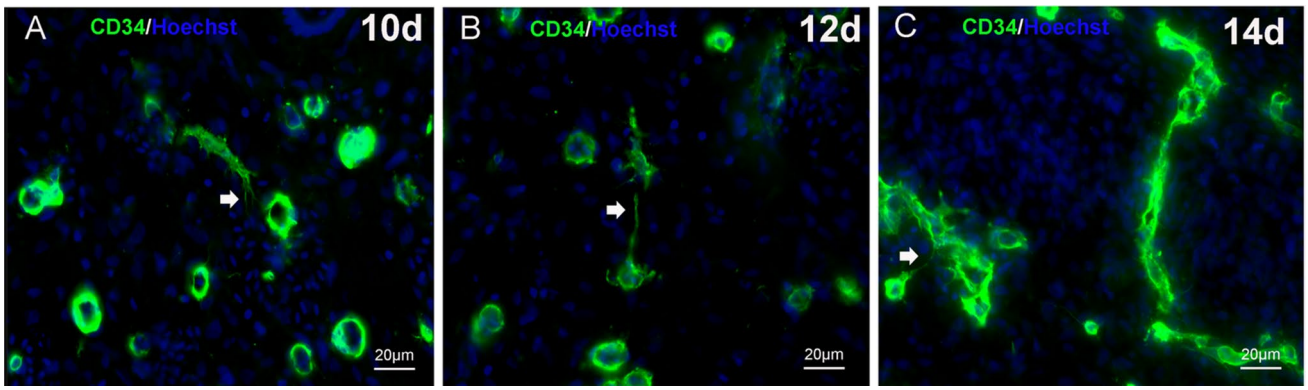

Fig. 3 Formation of a vasculature network from days 10–14**.** Transverse sections through the blastema, co-labelled with CD34 and Hoechst dye, revealed the progressive development of a vasculature network in the blastema. **A** On day 10, the majority of regenerated capillary vessels were circular in shape, with occasional sprouting endothelial cells (arrow) observed. **B** By day 12, there was increased evidence for endothelial cell sprouting (arrow) suggesting active angiogenesis during regeneration. **C** By day 14, the regenerating vessels were increasingly inter-connected and had developed into capillary network. Scale bar represents 20 μm

detect the vasculature. Comparison of Tuj1 staining patterns in rostral and caudal tails in transverse sections of regenerate tails on 14th day post amputation, showed that in tissues rostral to the amputation plane, Tuj1 signals were clearly detectable in the spinal cord and dorsal root ganglia (Fig. 4A, B) and various positive signals, representing peripheral nerves scattered in surrounding tissues. By contrast, the spinal cord and ganglia were absent in the regenerate tail caudal to the amputation plane (Fig. 4C, D) with Tuj1 signals limited to the ependymal tube, indicative of descending axons from the rostral neural tissues, and dispersed in the regenerate blastema tissues. This pattern of axon staining is consistent with the pattern of tail re-innervation described in another species of lizard, *Anolis carolinensis* (Tokuyama et al. 2018).

Examination of Tuj1 signals in longitudinal sections of the regenerating tail from the 4th to 14th day (Fig. 5) revealed that the nerve fibers reached the most distal end of the regenerated tissue on day 7 (Fig. 5D), including the overlying wound epithelium (Fig. 5E, F), suggesting rapid innervation of the early blastema. At day 10, the nerve fibers can be seen entering the growing blastema and as the blastema grew from days 12 to 14, nerve fibers were detected extending to the tip of the blastema at each stage (Fig. 5G–L).

To examine if there was a relationship between the growing nerves and neovascularization we investigated the spatial relationship between axons and newly formed vessels in longitudinal sections, co-labelled with Tuj1 and CD34. In all sections, nerves and vessels appeared to be separately located, with the separate signals widely scattered in the blastema (Fig. 5). To examine the dynamics of neovascularization and reinnervation, we quantified the numbers of vessel and nerve bundle profiles in transverse sections of the regenerating tails at days 10, 12 and 14 post amputation (Fig. 6). On day 10, there were numerous vessels with a typical regular rounded profile (Fig. 6A, B), but on days 12 and 14 this increasingly changed to significantly fewer, more elongated and ramified profiles (Fig. 6C–G). These results indicate that the numbers of vessels peak on the 10th day after amputation, and thereafter transform into a network by remodeling of endothelial cells. By contrast, the nerve

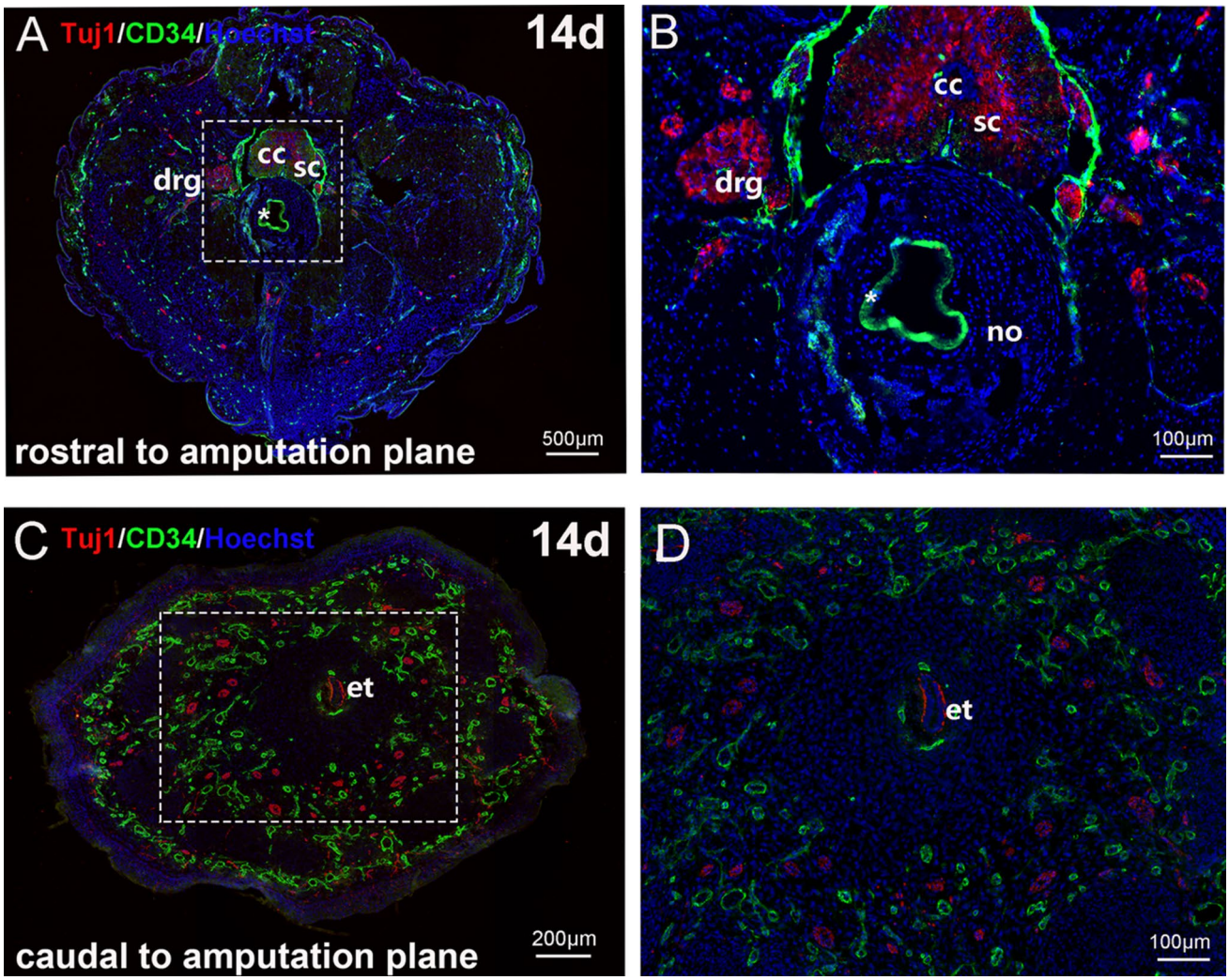

Fig. 4 The innervation pattern in rostral and caudal regions of regenerating tails on 14th day post amputation. Transverse sections through regions rostral (**A**, **B**) and caudal (**C**, **D**) to the amputation plane, co-labelled with antibodies to Tuj1 and CD34 and Hoechst dye. **A**, **B** In the rostral region, the spinal cord and dorsal root ganglion (DRG) were labelle with Tuj1 antibody in tissue rostral to amputation plane, and the nerve fibers were dispersed in the peripheral tissues. **B** shows an enlarged view of boxed area in **A**. The CD34 staining of the notochord (*) is non-specific. The results proposed that the association of vessels with nerves was not evident in our study. **C**, **D**. In the distal region, the spinal cord and DRG were absent and the nerve fibers were scattered throughout the blastema tissue, and associated with the ependymal tube. Scale bar represents 500 μm in **A**, 200 μm in **C**, and 100 μm in **B** and **D**. *cc* central canal, *drg* dorsal root ganglion, *et* ependymal tube, *no* notochord, *sc* spinal cord

density gradually and significantly increased from days 10 to 14 (Fig. 6G, H).

The satellite cells are activated during myogenesis of regenerated tail

Tail regeneration in lizards is thought to be mediated through the activation of stem/progenitor cells rather than by dedifferentiation of mature tissues (Fisher et al. 2012; Hutchins et al. 2014). In the present study, we observed the process of muscle regeneration by using a myosin heavy chain (MHC) antibody as a marker for muscle fibers. Fragmented muscle fibers, labelled with MHC antibody, were present in the region proximal to the amputation site on the 4th day post amputation (Supplementary Fig. S3A–C), but MHC signals were absent from the blastema on the 7th, 10th and 12th days (Supplementary Fig. S3G–L). The first evidence for muscle formation was observed as aggregations of MHC-positive cells aligning from proximal to distal of the regenerated tail on the 14th day (Fig. 7A–C). We further detected the musculature tissue in the cross section of the samples on the 14th day and demonstrated that regenerated muscle cells formed circular muscle bundles that were concentrically arranged around the central ependymal tube (Fig. 7D). Double labelling with an antibody to growth associated protein 43 (GAP43), which is expressed at high levels in regenerating axons, showed that the regenerated nerves were in close association with these muscle bundles (Fig. 7D).

To investigate whether there is muscle satellite cell activation during regeneration, we examined the expression of both PAX3 and PAX7 levels at different time points by western blots of regenerate blastema from day 0 to day 14 (Fig. 8). While PAX7 levels increased progressively from day 0 to day 14 (Fig. 8A, C), PAX3 expression appeared to peak at days 7–10 and then declined rapidly by day 14 to levels similar to day 0 (Fig. 8A, B). As the samples prepared for western blot contained both tissues rostral and caudal to the amputation plane, we further examined the spatial distribution of PAX3 by immunofluorescence, together with proliferating cell nuclear antigen (PCNA) to label active cell cycle on the 10th day post amputation. We found PAX3 and PCNA double-positive cells in the original tissue rostral to the amputation plane, which suggested satellite cell proliferation in the remaining muscles proximal to the amputation plane (Fig. 9A–D). However, PAX3 signal was not observed in the regenerated tissue caudal to the amputation plane (Fig. 9E–H). Unfortunately, immunofluorescence experiments with the PAX7 antibody failed to detect any signal, suggesting that this antibody does not recognize *Gekko japonicus* PAX7 in sections under the conditions used in this study.

Discussion

Lizards are amniotes with intermediate regenerative ability between that of amphibians (anamniotes) and homeothermic amniotes (birds and mammals) (Bely and Nyberg 2010). The descriptive and mechanistic investigation about the tail regeneration in lizards has grown rapidly in recent years. Morphological studies of the well-regenerated vessels and nerves have been documented in *Anolis carolinensis* (Zika 1969), *Podarcis muralis* (Alibardi 2014) and *Eublepharis macularius* (McLean and Vickaryous 2011; Delorme et al. 2012). In this study, we described the initial neovascularization, innervation and myogenesis during the first 14 days of tail regeneration in *Gekko japonicus*. The results showed that neovascularization and innervation of the regenerate tail occurred as the blastema started to grow (days 4–10), whereas appearance of the musculature occurred much later (days 12–14).

Vascularization is prerequisite for the survival of the regenerated tissue. Similar to other species capable of appendage regeneration, these structures are not formed de novo but result from the outgrowth of remnant rostral tissues within the proximal (non-autotomized) portion of the tail. We found that the angiogenesis occurred extensively from day 7 to day 14, and capillary vessel density was

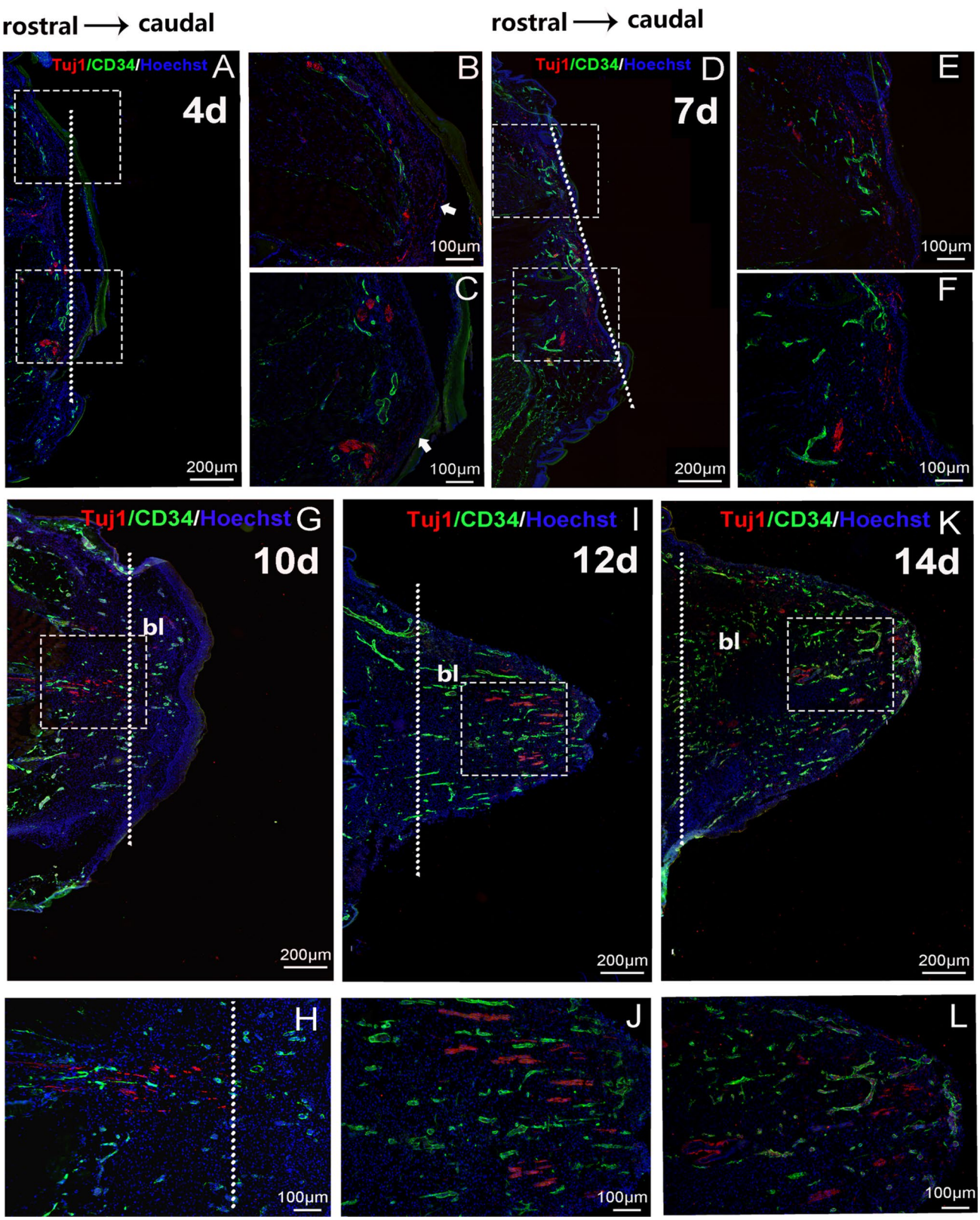
rostral ⟶ caudal
rostral ⟶ caudal
Tuj1/CD34/Hoechst
A
4d
B
C
100μm
200μm
100μm
Tuj1/CD34/Hoechst
D
7d
E
F
100μm
200μm
100μm
Tuj1/CD34/Hoechst
G
10d
bl
200μm
Tuj1/CD34/Hoechst
I
12d
bl
200μm
Tuj1/CD34/Hoechst
K
14d
bl
200μm
H
J
L
100μm
100μm
100μm

◂**Fig. 5** Progression of blastema innervation from 4 to 14 days. Longitudinal sections of blastema co-stained with Tuj1 antibody, CD34 antibody and Hoechst dye. **A**–**C** The nerve fibers could be observed on 4th day post amputation, indicating the innervation of the regenerating tissues occurred early. **B** and **C** show higher magnification views of the upper and lower boxed areas in **A**. The arrows indicated the Tuj1 signals in the distal wound epithelium. **D**–**F** By the 7th day post amputation, the nerve fibers were present in the overlying wound epithelium on 7th day in higher magnification views (**E** and **F**) of the boxed areas in **D**, nerve fibers are detectable in the overlying wound epithelium. **G**–**L** From 10 to 14 days post amputation, nerve fibers were increasingly evident in the distal blastema (bl). **H**, **J** and **L** show magnified views of the boxed areas in **G**, **I** and **K** respectively. Dashed lines indicate amputation plane. Scale bars represent 200 μm in **A**, **D**, **G**, **I** and **K**, 100 μm in **B**, **C**, **E**, **F**, **H**, **J** and **L**

highest on the 10th day after amputation. The early vascularization in blastema is different among the regeneration capable species. In urodeles, the early blastema is relatively avascular (Rageh et al. 2002), whereas in the leopard gecko (*Eublepharis macularius*), consistent with our study in *Gekko japonicus*, the early blastema is rich in blood vessels (McLean and Vickaryous 2011). In addition, we clearly showed capillary vessel extension, endothelial proliferation, sprouting and robust vessel remodeling, which were not addressed in previous studies. Co-labeling of vessels and nerves permitted comparison of the temporal and spatial progression of angiogenesis and innervation, and revealed that the blood vessel developed more quickly in the first 10 days of regeneration. However subsequent events, such as pericyte covering and differentiation of arteries and veins requires further investigation.

It has long been debated whether muscle regeneration in appendages involves resident adult stem cells or dedifferentiated mature cells. Studies in two salamander species, showed an unexpected evolutionary diversity in muscle regeneration. In the newt, *Notophthalmus viridescens,* muscle dedifferentiation made a significant contribution to muscle regeneration, whereas in the axolotl, *Ambystoma mexicanum*, PAX7-positive satellite cells were the main contributor to limb muscle regeneration (Sandoval-Guzmán et al. 2014). Similarly, in a previous study of muscle regeneration in the lizard, *Anolis carolinensis*, PAX7-positive satellite cells could be induced to fuse into multinucleated myotubes, which indicated the essential role of satellite cell activation during muscle regeneration in lizard (Hutchins et al. 2014). Morphologically, the early regenerating muscles consisted of many symmetrically arranged cellular aggregates, without the epaxial and hypaxial organization of the original tail. We found that regeneration of muscle occurred relatively late, with MHC + cells only detected on the 14th day post amputation. To investigate whether stem/progenitor cell activation or original muscle differentiation might begin earlier, we examined the expression of PAX3 and PAX7, which are paralogous transcription factors with overlapping roles in myogenic specification. PAX7 is maintained in satellite cells and proliferating myoblasts, while PAX3 has unique functions during embryonic development (Kang and Krauss 2010; Comai and Tajbakhsh 2014). Intriguingly, both factors increased in expression during blastema growth with PAX3 expression peaking on days 7–10 and PAX7 on day 14, which is consistent with a previous transcriptomic study of tail regeneration in *Anolis carolinensis* showing increased PAX7 expression in the proximal segment. Moreover, the PAX7-positive satellite cells in *Anolis carolinensis* showed a level of multipotency, differentiating to form cartilage and skeletal muscle (Palade et al. 2018). By immunofluorescence, we observed the proliferation of PAX3 positive cells in the tissue rostral to the plane of amputation, which suggested that satellite cells were activated in original tissue. However, while PAX3 was reported to drive the migration of stem/progenitor cells during development (Crist et al. 2009), we did not detect PAX3 positive cells in the caudal regenerate blastema at any stage up to 14 days post amputation. We speculate that PAX3 may be turned off or replaced by PAX7 expression once cells enter the blastema, which we unfortunately could not confirm with the antibodies available. The fate of the progeny from dividing PAX3 positive cells remains to be determined and the underlying mechanism of how

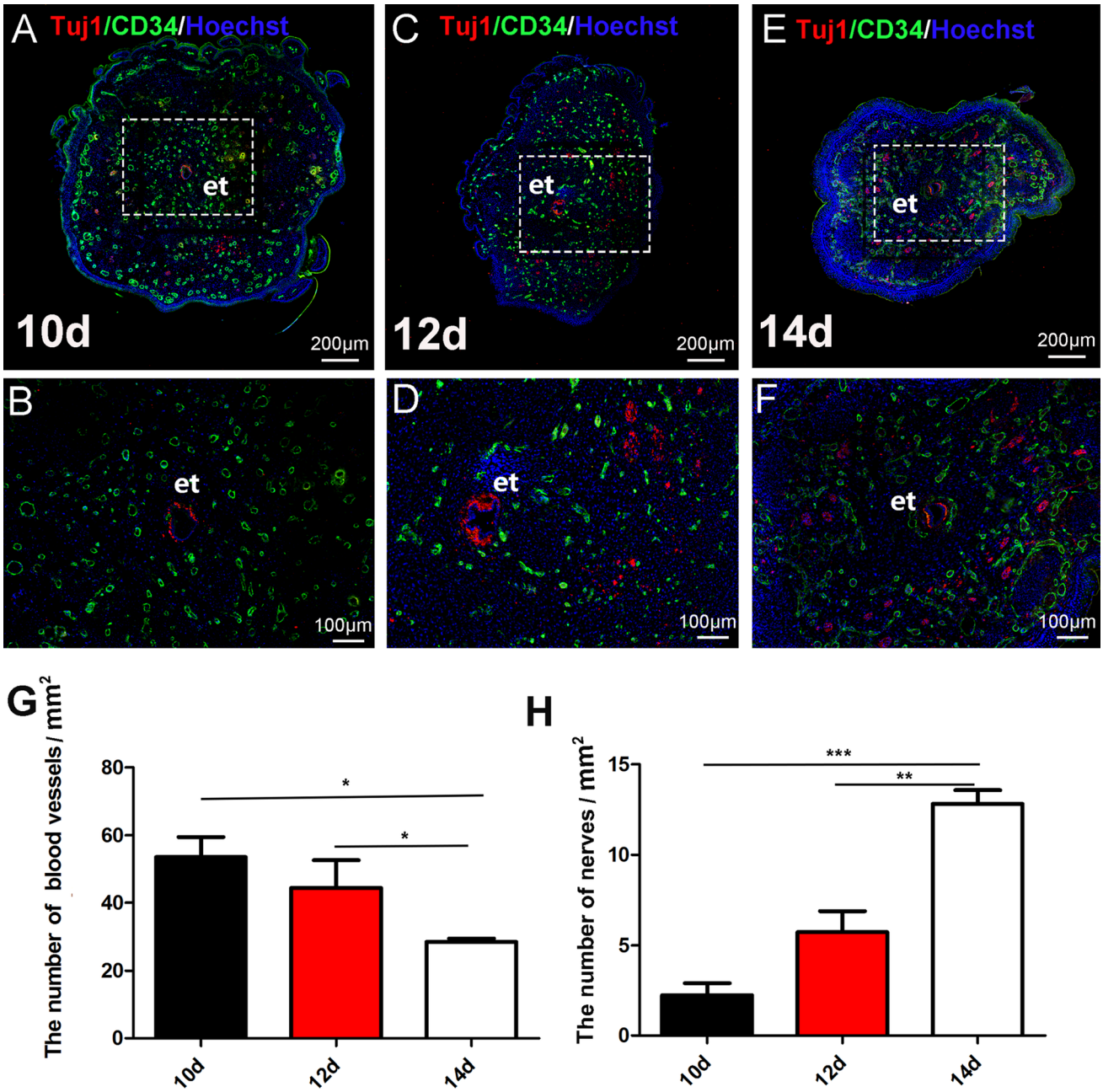

Fig. 6 Progression of blastema innervation and vascularization from 10 to 14 days. Transverse sections through the blastema at 10 (**A**, **B**), 12 (**C**, **D**) and 14 days (**E**, **F**) post amputation, showing regenerating blood vessels labelled with CD34 (green) and nerve tissues labelled with Tuj1 (red). **A**, **B** At 10 days, the regenerated vessels showed numerous round profiles and there were only sparse nerve bundles in the blastema with nerve fibers observed around ependymal tube (et). **B** is the enlarged view of boxed area in **A**. **C**, **D** On day 12, vessels increasingly appeared as elongated profiles and there were increased number of nerve fiber profiles. **D** is the enlarged view of boxed area in **C**. **E**, **F** By day 14, the capillary vessels increasingly appeared to form a network and nerve fiber bundles were even more numerous. **F** is the enlarged view of boxed area in **E**. **G** Quantification of vessel profiles revealed significant decreases ($*p < 0.05$) from days 10–14 post amputation. **H** Quantification of nerve profiles revealed significant increases from days 10–14 ($***p < 0.001$) and from days 12–14 ($**p < 0.01$) post amputation. All data were from three independent assay. Scale bar represents 200 μm in **A**, **C** and **E**, 100 μm in **B**, **D** and **F**

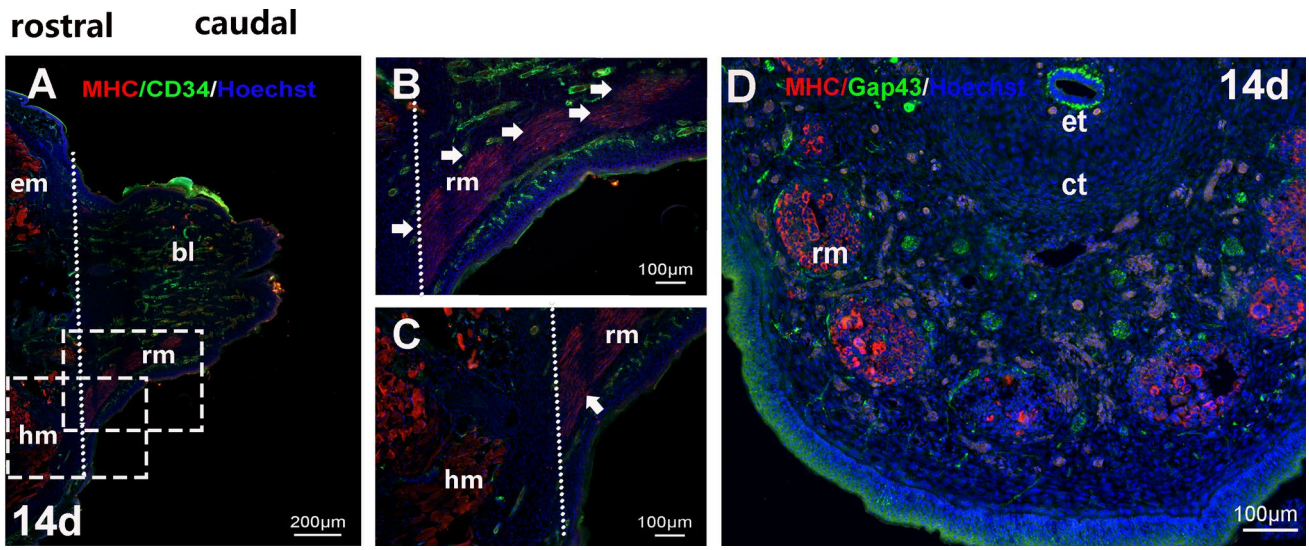

Fig. 7 Myogenesis of the regenerated tail. **A**–**C** In longitudinal sections of the regenerating tail on 14th day post amputation, the epaxial (em) and hypaxial (hm) muscles in the rostral stump were clearly labelled with the myosin heavy chain (MHC) antibody. The regenerating muscles (rm) were observed to align rostro-caudally in the blastema (bl). **B** and **C** are enlarged view of upper and lower boxed area in **A**, which showed regenerated muscle bundles aligned rostro-caudally (**B**) and rostral muscles adjacent to amputation plane (**C**). The arrows indicate regenerated muscles. **D** In transverse sections of the blastema at 14 days, the newly formed muscle tissues were arranged concentrically around the ependymal tube (et) and newly formed cartilage tube (ct). Co-labeling of sections with an antibody to growth associated protein 43 (GAP43) revealed nerve fibers innervating the regenerated muscles. Dashed lines in **A**–**C** indicate amputation plane. Scale bar represents 200 μm in **A**, 100 μm in **B**–**D**

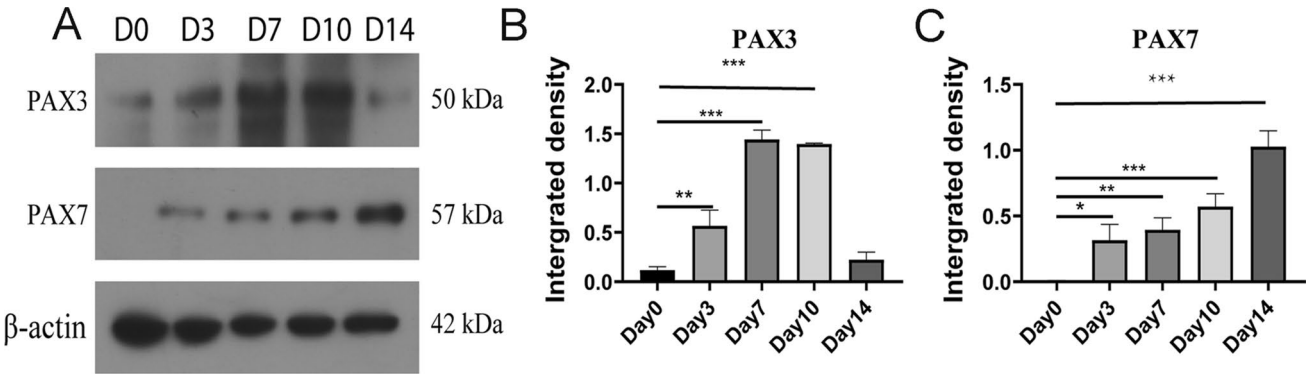

Fig. 8 Expression of PAX3 and PAX7 during tail regeneration. **A** Western blots of extracts from regenerating tails from days 0–14 showed continuously increased PAX7 expression until 14th day. By contrast, PAX3 expression peaked on day 10 and diminished on day 14. **B**, **C** Quantification of western blots confirmed statistically significant changes in expression for PAX3 from day 0 to days 3 (**$p < 0.01$), 7 and 10 (***$p < 0.001$) and significant increases at all time points (days 3–14) when compared to day 0 (One-way ANOVA; *$p < 0.05$, **$p < 0.01$, ***$p < 0.001$) vs. control). All data were obtained from 3 independent experiments

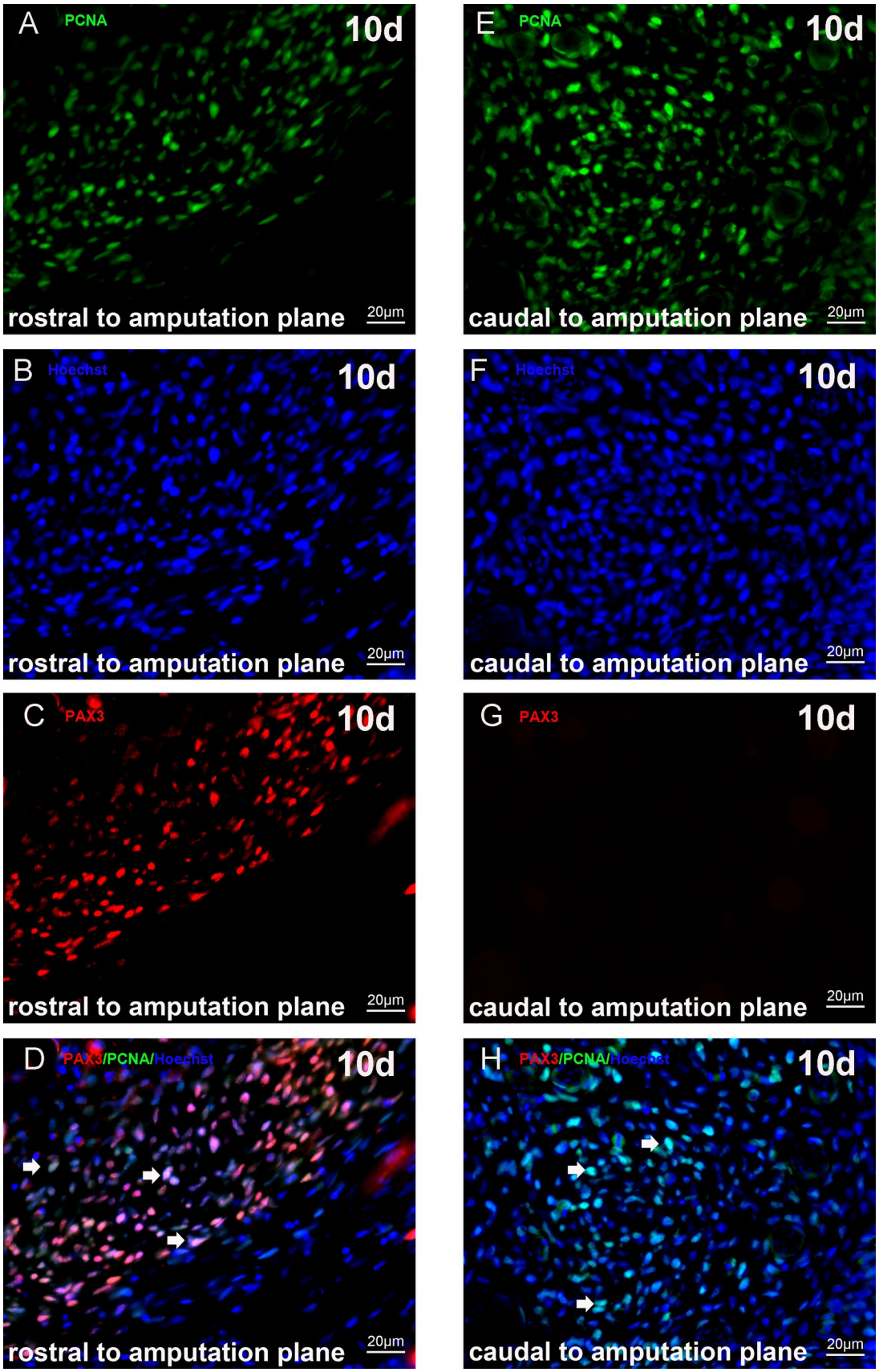
A PCNA 10d
rostral to amputation plane 20μm
E PCNA 10d
caudal to amputation plane 20μm
B Hoechst 10d
rostral to amputation plane 20μm
F Hoechst 10d
caudal to amputation plane 20μm
C PAX3 10d
rostral to amputation plane 20μm
G PAX3 10d
caudal to amputation plane 20μm
D PAX3/PCNA/Hoechst 10d
rostral to amputation plane 20μm
H PAX3/PCNA/Hoechst 10d
caudal to amputation plane 20μm

◂**Fig. 9** PAX3 expression is localized to the rostral regions of the regenerating tail. **A**–**D** In transverse sections rostral to amputation plane, PAX3 immunofluorescence was detected in hypaxial tissue. Co-labelling with Hoechst dye (**B**) and with an antibody for PCNA (**C**) revealed that many of these $PAX3^+$ cells were proliferating (**D**, arrows). **E**–**H** While proliferating $PCNA^+$ cells were abundant in regenerating tissues caudal to amputation plane, PAX3 positive cells were not observed. Scale bar represents 20 µm in all panels

muscle precursors migrate and contribute to tail regeneration requires further study.

Supplementary Information The online version contains supplementary material available at https://doi.org/10.1007/s10735-021-10032-y.

Acknowledgements This work was supported by National Natural Science Foundation of China (Grant No. 31970412, 31472004 and 31071874); Natural science foundation of Jiangsu province (Grant No. BK20191446); the Priority Academic Program Development (PAPD) of Jiangsu Higher Education Institutions.

Declarations

Conflict of interest All authors declare no conflict of interest.

References

Alibardi L (2014) Histochemical, biochemical and cell biological aspects of tail regeneration in lizard, an amniote model for studies on tissue regeneration. Prog Histochem Cytochem 48(4):143–244. https://doi.org/10.1016/j.proghi.2013.12.001

Alibardi L, Miolo V (1990) Fine observation on nerves colonizing the regenerating tail of the lizard *Podarcis sicula*. Histol Histopathol 5(4):387–396

Bely AE, Nyberg KG (2010) Evolution of animal regeneration: re-emergence of a field. Trends Ecol Evol 25(3):161–170. https://doi.org/10.1016/j.tree.2009.08.005

Comai G, Tajbakhsh S (2014) Molecular and cellular regulation of skeletal myogenesis. Curr Top Dev Biol 110:1–73. https://doi.org/10.1016/b978-0-12-405943-6.00001-4

Crist CG, Montarras D, Pallafacchina G, Rocancourt D, Cumano A, Conway SJ, Buckingham M (2009) Muscle stem cell behavior is modified by microRNA-27 regulation of Pax3 expression. Proc Natl Acad Sci USA 106(32):13383–13387. https://doi.org/10.1073/pnas.0900210106

Delorme SL, Lungu IM, Vickaryous MK (2012) Scar-free wound healing and regeneration following tail loss in the leopard gecko, *Eublepharis macularius*. Anat Record (hoboken, NJ: 2007) 295(10):1575–1595. https://doi.org/10.1002/ar.22490

Fisher RE, Geiger LA, Stroik LK, Hutchins ED, George RM, Denardo DF, Kusumi K, Rawls JA, Wilson-Rawls J (2012) A histological comparison of the original and regenerated tail in the green anole, *Anolis carolinensis*. Anat Record (hoboken, NJ: 2007) 295(10):1609–1619. https://doi.org/10.1002/ar.22537

Gilbert EA, Payne SL, Vickaryous MK (2013) The anatomy and histology of caudal autotomy and regeneration in lizards. Physiol Biochem Zool PBZ 86(6):631–644. https://doi.org/10.1086/673889

Haas BJ, Whited JL (2017) Advances in decoding axolotl limb regeneration. Trends Genet TIG 33(8):553–565. https://doi.org/10.1016/j.tig.2017.05.006

Hutchins ED, Markov GJ, Eckalbar WL, George RM, King JM, Tokuyama MA, Geiger LA, Emmert N, Ammar MJ, Allen AN, Siniard AL, Corneveaux JJ, Fisher RE, Wade J, DeNardo DF, Rawls JA, Huentelman MJ, Wilson-Rawls J, Kusumi K (2014) Transcriptomic analysis of tail regeneration in the lizard Anolis carolinensis reveals activation of conserved vertebrate developmental and repair mechanisms. PLoS ONE 9(8):e105004. https://doi.org/10.1371/journal.pone.0105004

Jiang M, Gu X, Feng X, Fan Z, Ding F, Liu Y (2009) The molecular characterization of the brain protein 44-like (Brp44l) gene of Gekko japonicus and its expression changes in spinal cord after tail amputation. Mol Biol Rep 36(2):215–220. https://doi.org/10.1007/s11033-007-9169-0

Kahn EB, Simpson SB Jr (1974) Satellite cells in mature, uninjured skeletal muscle of the lizard tail. Dev Biol 37(1):219–223. https://doi.org/10.1016/0012-1606(74)90181-x

Kang JS, Krauss RS (2010) Muscle stem cells in developmental and regenerative myogenesis. Curr Opin Clin Nutr Metab Care 13(3):243–248. https://doi.org/10.1097/MCO.0b013e328336ea98

Londono R, Wenzhong W, Wang B, Tuan RS, Lozito TP (2017) Cartilage and muscle cell fate and origins during lizard tail regeneration. Front Bioeng Biotechnol 5:70. https://doi.org/10.3389/fbioe.2017.00070

Lozito TP, Tuan RS (2015) Lizard tail regeneration: regulation of two distinct cartilage regions by Indian hedgehog. Dev Biol 399(2):249–262. https://doi.org/10.1016/j.ydbio.2014.12.036

McLean KE, Vickaryous MK (2011) A novel amniote model of epimorphic regeneration: the leopard gecko, *Eublepharis Macularius*. BMC Dev Biol 11:50. https://doi.org/10.1186/1471-213x-11-50

Morrison JI, Lööf S, He P, Simon A (2006) Salamander limb regeneration involves the activation of a multipotent skeletal muscle satellite cell population. J Cell Biol 172(3):433–440. https://doi.org/10.1083/jcb.200509011

Nacu E, Tanaka EM (2011) Limb regeneration: a new development? Annu Rev Cell Dev Biol 27:409–440. https://doi.org/10.1146/annurev-cellbio-092910-154115

Nowoshilow S, Schloissnig S, Fei JF, Dahl A, Pang AWC, Pippel M, Winkler S, Hastie AR, Young G, Roscito JG, Falcon F, Knapp D, Powell S, Cruz A, Cao H, Habermann B, Hiller M, Tanaka EM, Myers EW (2018) The axolotl genome and the evolution of key tissue formation regulators. Nature 554(7690):50–55. https://doi.org/10.1038/nature25458

Palade J, Djordjevic D, Hutchins ED, George RM, Cornelius JA, Rawls A, Ho JWK, Kusumi K, Wilson-Rawls J (2018) Identification of satellite cells from anole lizard skeletal muscle and demonstration of expanded musculoskeletal potential. Dev Biol 433(2):344–356. https://doi.org/10.1016/j.ydbio.2017.08.037

Payne SL, Peacock HM, Vickaryous MK (2017) Blood vessel formation during tail regeneration in the leopard gecko (*Eublepharis macularius*): the blastema is not avascular. J Morphol 278(3):380–389. https://doi.org/10.1002/jmor.20648

Pfefferli C, Jaźwińska A (2015) The art of fin regeneration in zebrafish. Regeneration (oxford, England) 2(2):72–83. https://doi.org/10.1002/reg2.33

Rageh MA, Mendenhall L, Moussad EE, Abbey SE, Mescher AL, Tassava RA (2002) Vasculature in pre-blastema and nerve-dependent blastema stages of regenerating forelimbs of the adult newt, *Notophthalmus viridescens*. J Exp Zool 292(3):255–266. https://doi.org/10.1002/jez.10015

Rakocevic J, Orlic D, Mitrovic-Ajtic O, Tomasevic M, Dobric M, Zlatic N, Milasinovic D, Stankovic G, Ostojić M, Labudovic-Borovic M (2017) Endothelial cell markers from clinician's perspective. Exp Mol Pathol 102(2):303–313. https://doi.org/10.1016/j.yexmp.2017.02.005

Sandoval-Guzmán T, Wang H, Khattak S, Schuez M, Roensch K, Nacu E, Tazaki A, Joven A, Tanaka EM, Simon A (2014) Fundamental

differences in dedifferentiation and stem cell recruitment during skeletal muscle regeneration in two salamander species. Cell Stem Cell 14(2):174–187. https://doi.org/10.1016/j.stem.2013.11.007

Semenza GL (2007) Vasculogenesis, angiogenesis, and arteriogenesis: mechanisms of blood vessel formation and remodeling. J Cell Biochem 102(4):840–847. https://doi.org/10.1002/jcb.21523

Simpson SB Jr. (1970) Studies on regeneration of the lizard's tail. Am Zool 10(2):157–165. https://doi.org/10.1093/icb/10.2.157

Stocum DL, Cameron JA (2011) Looking proximally and distally: 100 years of limb regeneration and beyond. Dev Dyn off Publ Am Assoc Anat 240(5):943–968. https://doi.org/10.1002/dvdy.22553

Tokuyama MA, Xu C, Fisher RE, Wilson-Rawls J, Kusumi K, Newbern JM (2018) Developmental and adult-specific processes contribute to de novo neuromuscular regeneration in the lizard tail. Dev Biol 433(2):287–296. https://doi.org/10.1016/j.ydbio.2017.10.003

Xu M, Wang T, Li W, Wang Y, Xu Y, Mao Z, Wu R, Liu M, Liu Y (2019) PGE2 facilitates tail regeneration via activation of Wnt signaling in *Gekko japonicus*. J Mol Histol 50(6):551–562. https://doi.org/10.1007/s10735-019-09847-7

Yokoyama H (2008) Initiation of limb regeneration: the critical steps for regenerative capacity. Dev Growth Differ 50(1):13–22. https://doi.org/10.1111/j.1440-169X.2007.00973.x

Zhou Y, Xu Q, Li D, Zhao L, Wang Y, Liu M, Gu X, Liu Y (2013) Early neurogenesis during caudal spinal cord regeneration in adult *Gekko japonicus*. J Mol Histol 44(3):291–297. https://doi.org/10.1007/s10735-012-9466-3

Zika JM (1969) A histological study of the regenerative response in a lizard, *Anolis carolinensis*. J Exp Zool 172(1):1–8. https://doi.org/10.1002/jez.1401720102

Publisher's Note Springer Nature remains neutral with regard to jurisdictional claims in published maps and institutional affiliations.